

Hidden multipolar orders of dipole-octupole doublets on a triangular lattice

Yao-Dong Li¹, Xiaoqun Wang^{2,4}, and Gang Chen^{1,3,4*}

¹State Key Laboratory of Surface Physics, Center for Field Theory and Particle Physics, Department of Physics, Fudan University, Shanghai 200433, People's Republic of China

²Department of Physics and Astronomy, Shanghai Jiao Tong University, Shanghai 200240, Peoples Republic of China

³Perimeter Institute for Theoretical Physics, Waterloo, Ontario N2L 2Y5, Canada and

⁴Collaborative Innovation Center of Advanced Microstructures, Nanjing, 210093, People's Republic of China

(Dated: August 26, 2016)

Motivated by the recent development in strong spin-orbit-coupled materials, we consider the dipole-octupole doublets on the triangular lattice. We propose the most general interaction between these unusual local moments. Due to the spin-orbit entanglement and the special form of its wavefunction, the dipole-octupole doublet has a rather peculiar property under the lattice symmetry operation. As a result, the interaction is highly anisotropic in the pseudospin space, but remarkably, is uniform spatially. We analyze the ground state properties of this generic model and emphasize the hidden multipolar orders that emerge from the dipolar and octupolar interactions. We clarify the quantum mutual modulations between the dipolar and octupolar orders. We predict the experimental consequences of the multipolar orders and propose the rare-earth triangular materials as candidate systems for these unusual properties.

Introduction.—In recent years, there has been an intensive interest in exploring electron systems that involve both strong spin-orbit coupling (SOC) and substantial electron correlations, especially in materials with heavy elements such as 5d transition metal elements and 4f rare-earth elements [1–4]. Because of the spatial orientation of the orbitals, the spin-orbit entanglement in strongly correlated Mott insulators often gives rise to rather complicated models that involve both spatial and spin anisotropies [2, 5–9]. While this is true for most spin-orbit-entangled moment, in this Letter, we propose a remarkably simple model for a peculiar spin-orbit-entangled doublet, namely “dipole-octupole doublet” (DO doublet) [10, 11] on a triangular lattice, and connect this model with the rare-earth based triangular lattice materials. Due to the multipolar nature of the interaction, this simple but realistic model, in a large parameter regime, realizes *hidden* magnetic multipolar orders and leads to unexpected experimental consequences.

The search for hidden order is an active field in the f electron systems [12]. The magnetic multipolar order has been proposed for URu_2Si_2 and NpO_2 , and various experimental evidence has been found [12–14]. Nevertheless, the precise nature of the multipolar orders in URu_2Si_2 and NpO_2 has not come to a consensus. It is partly because the complication and multitudes of the degree of freedom often prohibit the precise modeling of the multipolar interactions in these systems. In contrast, our model is a precise modeling of the multipolar interactions for the DO doublet systems and might be the simplest such model in the strong spin-orbit-coupled materials that realizes hidden multipolar orders [1, 12].

Three families of triangular lattice materials, MgYbGaO_4 [15–20], the isostructural ternary family RCd_3P_3 , RZn_3P_3 , RCd_3As_3 , RZn_3As_3 ($\text{R} = \text{Ce}, \text{Pr}, \text{Nd}, \text{Sm}$) [21–23], and $\text{R}_2\text{O}_2\text{CO}_3$ ($\text{R} = \text{Nd}, \text{Sm}, \text{Dy}$) [24], have recently been discovered. These materials contain

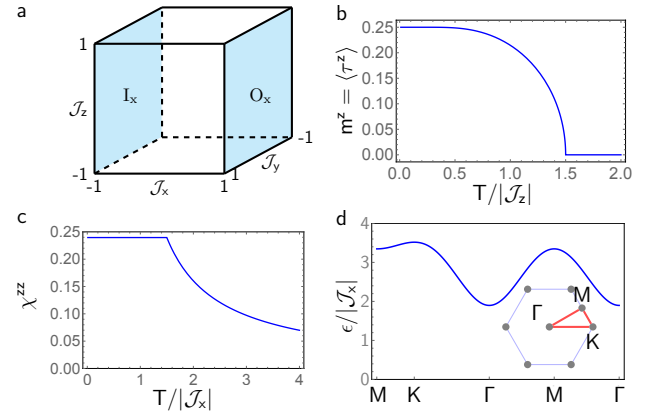


FIG. 1. (a) The six surfaces of the cuboid. I_μ (O_μ) refers to the inner (outer) surface with $J_\mu = -1$ ($J_\mu = 1$). We have marked the I_x and O_x surfaces. (b) The magnetization of the FD_z state on the I_z surface with $(J_x, J_y, J_z) = (-0.5, -0.2, -1)$ and $\theta = \pi/3$. The FD_z transition is at $T_d = 1.5|J_z|$. (c) Magnetic susceptibility χ^{zz} of the FO state on the I_x surface with $(J_x, J_y, J_z) = (-1, -0.2, -0.5)$ and $\theta = \pi/3$. The FO transition is at $T_o = 1.5|J_x|$. (d) Octupolar-wave excitation with the same parameters as in (c).

the rare-earth elements, whose 4f electrons involve strong SOC and strong correlations. The strong SOC entangles the total electron spin \mathbf{S} with the orbital angular momentum \mathbf{L} and leads to a total moment \mathbf{J} . Like the case in the rare-earth pyrochlores [25], the local D_{3d} crystal electric field (CEF) splits the $(2J+1)$ states into the crystal field states [16]. For a half-integer (integer) J , the CEF ground state is a Kramers' doublet (either a singlet or a non-Kramers' doublet). The ground state doublets define the low-temperature magnetic properties of the system. In the previous work, we proposed a generic anisotropic spin model for non-Kramers' doublets and the usual Kramers' doublets on a triangular

lattice [16]. Here we introduce a generic model for the DO Kramers' doublet on the triangular lattice [15, 16] and predict the experimental consequences of the hidden multipolar orders.

Dipole-octupole doublet.—The DO doublet is a special type of Kramers' doublet. It occurs when the crystal field ground state wavefunctions $|\Psi_{\pm}\rangle$ are linear superpositions of the states with $J^z = 3n/2$ where n is an odd integer. Unlike the usual Kramers doublets that transform as a two-dimensional irreducible representation of the D_{3d} point group [16], each state of the DO doublet transforms as a one-dimensional irreducible representation (Γ_5^+ or Γ_6^+) of the D_{3d} point group [10]. This crucial difference is most easy to be understood if one applies the 3-fold rotation along the z axis to these states. Under the 3-fold rotation, we have $\exp(-i\frac{2\pi}{3}J^z)|J^z = 3n/2\rangle = -|J^z = 3n/2\rangle$. Therefore, the wavefunctions of the DO doublet, $|\Psi_{\pm}\rangle$, stay invariant under this rotation except getting an overall minus sign, *i.e.*,

$$\exp(-i\frac{2\pi}{3}J^z)|\Psi_{\pm}\rangle = -|\Psi_{\pm}\rangle. \quad (1)$$

In contrast, for the usual Kramers' doublet, the two states would mix with each other under this rotation. The degeneracy of the DO doublet is protected by time reversal symmetry that switches the two states. This special doublet has been found in various neodymium (Nd) pyrochlores [26–32], dysprosium (Dy) pyrochlore [33], osmium (Os) pyrochlore [34, 35], erbium (Er) and ytterbium (Yb) spinels [32, 36], and $\text{Ce}_2\text{Sn}_2\text{O}_7$ [37]. We expect the DO doublet should occur in some of the rare-earth triangular materials, especially since these rare-earth ions experience the same D_{3d} crystal field environment.

Generic pseudospin model on a triangular lattice.—Here we explain the interaction between the DO doublets on a triangular lattice. Due to the two-fold degeneracy of the DO doublet, we introduce the pseudospin operators that act on this DO doublet, $\tau^+ = |\Psi_+\rangle\langle\Psi_-|$, $\tau^- = |\Psi_-\rangle\langle\Psi_+|$, $\tau^z = \frac{1}{2}|\Psi_+\rangle\langle\Psi_+| - \frac{1}{2}|\Psi_-\rangle\langle\Psi_-|$, where $\tau^{\pm} \equiv \tau^x \pm i\tau^y$. To obtain the exchange interaction, we start with the symmetry properties of the pseudospins under the space group symmetry.

For all the three families of rare-earth triangular lattice materials [15–24], the space group is either $R\bar{3}m$ or $P6_3mmc$. As all rare-earth ions in these materials have a layered triangular structure and the interlayer separation is much larger than the intralayer lattice constant, it is sufficient to just keep the interaction within the triangular layer and ignore the interlayer couplings. As far as the space group symmetry is concerned, we only need to retain the symmetry generators that operate within each triangular layer. It turns out that, for a single triangular layer, both $R\bar{3}m$ and $P6_3mmc$ space groups give a three-fold rotation around the z axis, C_3 , a two-fold rotation about the diagonal direction, C_2 , a site inversion symmetry I , and two lattice translations, T_x and T_y . The

symmetry operation on $\tau_{\mathbf{r}}^{\mu}$ is given as [38]

$$\begin{cases} C_3 : \tau_{\mathbf{r}}^x \rightarrow \tau_{C_3(\mathbf{r})}^x, \tau_{\mathbf{r}}^y \rightarrow \tau_{C_3(\mathbf{r})}^y, \tau_{\mathbf{r}}^z \rightarrow \tau_{C_3(\mathbf{r})}^z, \\ C_2 : \tau_{\mathbf{r}}^x \rightarrow \tau_{C_2(\mathbf{r})}^x, \tau_{\mathbf{r}}^y \rightarrow -\tau_{C_2(\mathbf{r})}^y, \tau_{\mathbf{r}}^z \rightarrow -\tau_{C_2(\mathbf{r})}^z, \\ I : \tau_{\mathbf{r}}^x \rightarrow \tau_{I(\mathbf{r})}^x, \tau_{\mathbf{r}}^y \rightarrow \tau_{I(\mathbf{r})}^y, \tau_{\mathbf{r}}^z \rightarrow \tau_{I(\mathbf{r})}^z, \\ T_x : \tau_{\mathbf{r}}^x \rightarrow \tau_{T_x(\mathbf{r})}^x, \tau_{\mathbf{r}}^y \rightarrow \tau_{T_x(\mathbf{r})}^y, \tau_{\mathbf{r}}^z \rightarrow \tau_{T_x(\mathbf{r})}^z, \\ T_y : \tau_{\mathbf{r}}^x \rightarrow \tau_{T_y(\mathbf{r})}^x, \tau_{\mathbf{r}}^y \rightarrow \tau_{T_y(\mathbf{r})}^y, \tau_{\mathbf{r}}^z \rightarrow \tau_{T_y(\mathbf{r})}^z. \end{cases} \quad (2)$$

Since the $4f$ electron wavefunction is very localized, we only need to keep the nearest-neighbor interactions. The most general nearest-neighbor model, allowed by the above symmetries, is given as

$$H_0 = \sum_{\langle\mathbf{r}\mathbf{r}'\rangle} [J_x \tau_{\mathbf{r}}^x \tau_{\mathbf{r}'}^x + J_y \tau_{\mathbf{r}}^y \tau_{\mathbf{r}'}^y + J_z \tau_{\mathbf{r}}^z \tau_{\mathbf{r}'}^z + J_{yz} (\tau_{\mathbf{r}}^y \tau_{\mathbf{r}'}^z + \tau_{\mathbf{r}}^z \tau_{\mathbf{r}'}^y)]. \quad (3)$$

Here we give a few comments on this model. First of all, the pseudospin interaction is anisotropic in the pseudospin space because of the spin-orbit entanglement in the DO doublet. What is surprising is that the interaction is spatially uniform and is identical for every bond orientation. This is unusual since the orbitals have orientations. This remarkable spatial property comes from the peculiar symmetry property of the DO doublet in Eq. (2). Secondly, there exists a crossing coupling between τ^y and τ^z because τ^y and τ^z transform identically and behave like the magnetic dipole moments under the space group. Thirdly, there is no crossing coupling between τ^x and τ^y or τ^z because τ^x transforms as an octupole moment under the space group. This holds even for further neighbor interactions [39]. The J_x interaction is the interaction between the octupole moments.

Another remarkable property of the DO doublet is the infinite anisotropy in the Landé g -factor when it couples to an external magnetic field. After including the Zeeman term, we have the full Hamiltonian $H = H_0 - h \sum_{\mathbf{r}} \tau_{\mathbf{r}}^z$. Due to the spatial uniformity of the interaction, we are able to implement a rotation by an angle θ around the x direction in the pseudospin space and eliminate the crossing coupling between τ^y and τ^z . The reduced model is given as

$$H = \sum_{\langle\mathbf{r}\mathbf{r}'\rangle} [\mathcal{J}_x T_{\mathbf{r}}^x T_{\mathbf{r}'}^x + \mathcal{J}_y T_{\mathbf{r}}^y T_{\mathbf{r}'}^y + \mathcal{J}_z T_{\mathbf{r}}^z T_{\mathbf{r}'}^z] - h \sum_{\mathbf{r}} [\cos \theta T_{\mathbf{r}}^z + \sin \theta T_{\mathbf{r}}^y], \quad (4)$$

where $T^x = \tau^x$, $T^y = \tau^z \sin \theta + \tau^y \cos \theta$, $T^z = \tau^z \cos \theta - \tau^y \sin \theta$, and $\mathcal{J}_x, \mathcal{J}_y, \mathcal{J}_z$ are defined in the Supplementary information. Note both T^y and T^z behave like dipole moments. Like the XYZ model on the pyrochlore lattice [10, 11], this model does not have a sign problem for quantum Monte Carlo simulation in a large parameter regime, and this is valid on any other lattices such as the 3D FCC lattice where DO doublets could exist [8].

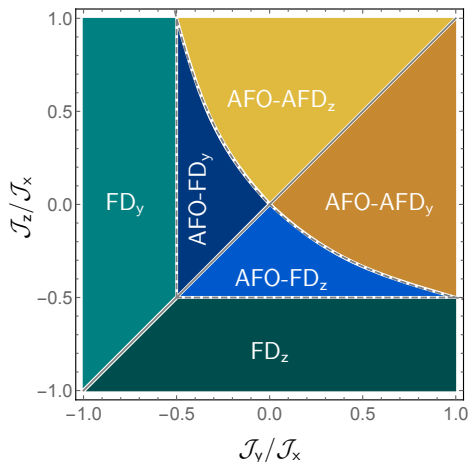


FIG. 2. (Color online.) The phase diagram on the O_x surface ($J_x = 1$). Solid (dashed) lines indicate first (continuous) order phase transitions.

Hidden ferro-octupolar orders.—We now explain the hidden multipolar orders of the model in Eq. (4). We start with the parameter regime on the I_z surface with $J_z = -1$ (see Fig. 1a). This regime simply gives a conventional ferromagnetic ground state with a uniform $\langle T^z \rangle$. Since T^z is a dipole moment, this state is dubbed ferro-dipolar (FD_z) state, where the subindex z refers to the direction of the dipole moment. With a ferromagnetic dipole moment, this state can be readily confirmed in a magnetization measurement.

The reduced model in Eq. (4) has an interesting permutation structure. Using the result on the I_z surface, we can generate the ground states on the I_y surface with $J_y = -1$ and the I_x surface with $J_x = -1$. As the FD_y order of the I_y surface shares the same symmetry as the FD_z order of the I_z surface, we do not give a repeated discussion here. Although the permutation trick to relate different regimes seems simple, the physics on the I_x surface is rather special and unconventional, and it is this distinction that we clarify below. Clearly, as $\langle T^x \rangle$ is uniform and non-zero on the I_x surface, time reversal symmetry is explicitly broken and the ground state is a ferromagnetic state. As we compute within the mean-field theory in the Supplementary Information and show in Fig. 1, however, the magnetic susceptibility does not show any divergent behavior. This is very different from what we would naively expect for an usual ferromagnetic state. The order parameter $\langle T^x \rangle$ is an octupole moment and does not couple linearly to the external magnetic field. Therefore, it is hidden in the usual magnetization measurement.

Despite its invisibility in the usual thermodynamic measurements, one could instead search for the evidence of the octupolar order by other experimental probes. Since the octupolar order explicitly breaks time reversal

symmetry, polar Kerr effect could be used to detect the time reversal symmetry breaking [40]. Moreover, inside the FO phase, the dipole moment τ^z flips the octupole moment and creates octupolar-wave excitations. As τ^z directly couples to the neutron spin, the octupolar-wave excitation can be directly detected by an inelastic neutron scattering experiment. Using the Holstein-Primakoff boson transformation [38], we obtain the octupolar-wave dispersion,

$$\omega_{\mathbf{k}} = [\mathcal{J}_y \sum_i \cos[\mathbf{k} \cdot \mathbf{a}_i] - 3\mathcal{J}_x]^{\frac{1}{2}} \times [\mathcal{J}_z \sum_i \cos[\mathbf{k} \cdot \mathbf{a}_i] - 3\mathcal{J}_x]^{\frac{1}{2}}, \quad (5)$$

where the summation is over the three nearest neighboring vectors $\mathbf{a}_1 = (1, 0)$, $\mathbf{a}_2 = (-1/2, \sqrt{3}/2)$, and $\mathbf{a}_3 = (-1/2, -\sqrt{3}/2)$. One should observe a well-defined octupolar wave excitation below the FO transition despite the absence of ordering in the magnetization measurement. This mode is generically gapped because of the low symmetry of the model. We depict the octupolar wave excitation in Fig. 1d.

Hidden antiferro-octupolar orders.—Here we consider the parameter regimes where the dominant interaction is antiferromagnetic. We focus on the O_x surface where the octupolar exchange coupling \mathcal{J}_x is antiferromagnetic and dominant. For the O_y and the O_z surfaces, one can apply the permutation on the O_x surface and generate the phase diagrams and the relevant phases. In the absence of the exchange couplings \mathcal{J}_y and \mathcal{J}_z , the Ising exchange interaction \mathcal{J}_x is highly frustrated on the triangular lattice. Any state that satisfies the “2-plus 1-minus” or “2-minus 1-plus” condition for the T^x configuration on every triangle is the ground state. Therefore, the ground state is extensively degenerate.

In the XXZ limit of the model with $\mathcal{J}_y = \mathcal{J}_z$, the weak \mathcal{J}_y and \mathcal{J}_z exchanges allows the system to tunnel quantum mechanically within the degenerate ground state manifold and lifts the degeneracy via an order by quantum disorder effect [41–44]. It is well established that the system develops a supersolid order in a large parameter regime of the XXZ limit. With a supersolid order, the system spontaneously breaks the $U(1)$ symmetry with $\langle T^{y,z} \rangle \neq 0$ and the translation symmetry with $\langle T^x \rangle \neq 0$. Moreover, the system has a 3-sublattice magnetic structure in the supersolid phase.

To obtain the phase diagram away from the XXZ limit, we implement a self-consistent mean-field theory by assuming a 3-sublattice structure for the mean-field ansatz [38]. Via the mean-field decoupling, we have

$$H_{\text{MF}} = 3 \sum_{\mathbf{r} \in \text{A}} \sum_{\mu} [\mathcal{J}_{\mu}(m_{\text{B}}^{\mu} + m_{\text{C}}^{\mu}) T_{\mathbf{r}}^{\mu}] + 3 \sum_{\mathbf{r} \in \text{B}} \sum_{\mu} [\mathcal{J}_{\mu}(m_{\text{C}}^{\mu} + m_{\text{A}}^{\mu}) T_{\mathbf{r}}^{\mu}]$$

$$\begin{aligned}
& + 3 \sum_{\mathbf{r} \in C} \sum_{\mu} [\mathcal{J}_{\mu} (m_{\Lambda}^{\mu} + m_{\Lambda}^{\mu}) T_{\mathbf{r}}^{\mu}] \\
& - h \sum_{\mathbf{r}} [\cos \theta T_{\mathbf{r}}^z + \sin \theta T_{\mathbf{r}}^y], \quad (6)
\end{aligned}$$

where $m_{\Lambda}^{\mu} = \langle T_{\mathbf{r}}^{\mu} \rangle$ is determined self-consistently for $\mathbf{r} \in \Lambda$ -th sublattice with $\Lambda = A, B, C$. Such a mean-field theory captures both the uniform state and the 3-sublattice state. The mean-field phase diagram is depicted in Fig. 2. The FD_y and the FD_z phases are the previously mentioned ferro-dipolar orders with a uniform $\langle T^y \rangle \neq 0$ and $\langle T^z \rangle \neq 0$, respectively. There is no octupolar order here. It is the considerable ferro-dipolar interaction in these regions that competes with the antiferro-octupolar interaction and completely suppresses any octupolar order.

In region AFO-FD_y (AFO-FD_z) where the transverse exchange \mathcal{J}_y (\mathcal{J}_z) is reduced, the octupole moment T^x orders antiferromagnetically and develops a 3-sublattice structure while the dipole moment T^y (T^z) remains ferromagnetically ordered (see Fig. 3a). Therefore, the phase is listed as AFO-FD_y (AFO-FD_z). In these regions, the weak ferro-dipolar interaction allows the system to fluctuate within the extensively degenerate ground state manifold of the predominant antiferro-octupolar interaction and breaks the degeneracy, leading to the 3-sublattice octupolar order. The background 3-sublattice octupolar order further modulates the ferro-dipolar order and renders the 3-sublattice structure to the ferro-dipolar order. Such a mutual modulation between unfrustrated ferro-dipolar and the frustrated antiferro-octupolar interactions is in fact a *quantum effect*, and cannot occur in a classical spin system with the same model.

The 3-sublattice structure of the ferro-dipolar order is a direct consequence of the underlying antiferromagnetic octupolar order. This 3-sublattice structure, however, is completely hidden in the magnetization measurement that merely gives a finite net magnetization. To reveal the underlying 3-sublattice structure, one would need local probes such as NMR and μSR . The nuclear spin and muon spin only couple to the dipolar moment, and probe the local dipolar orders of different sublattices. Alternatively, the elastic neutron scattering directly probes the structure of the dipolar orders, and would observe the magnetic Bragg peaks at the Γ point that corresponds to the uniform part of the dipolar order as well as the K points that correspond to the 3-sublattice modulation of the dipolar order. Besides the static properties, the system supports three bands of excitations because of the 3-sublattice structure of the octupolar order. This can be well-observed in an inelastic neutron scattering measurement. We plot the the magnetic excitations in Fig. 3c.

In region AFO-AFD_y (AFO-AFD_z), the transverse coupling \mathcal{J}_y (\mathcal{J}_z) is antiferromagnetic. The system is therefore frustrated, and due to frustration the 3-

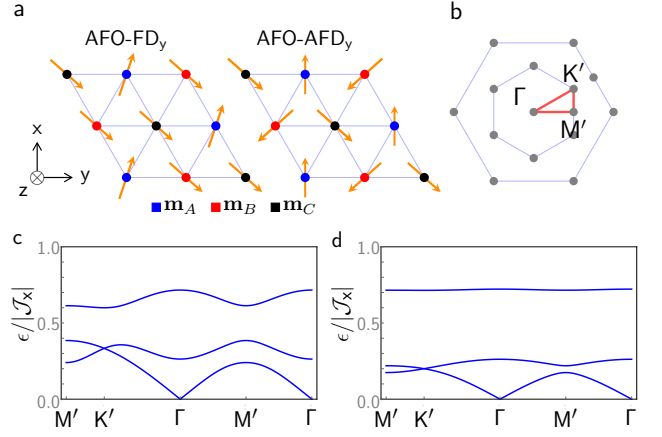


FIG. 3. (a) The ordering pattern in the AFO-FD_y and AFO-AFD_y phases. The local moments are in the xy -plane of the pseudospin space. The pseudospin configurations of phases across the diagonal line of the phase diagram in Fig. 2 are related by interchanging y and z components of \mathbf{m} . Inset is the coordinate system for the pseudospins. (b) The original Brillouin zone and the folded Brillouin zone due to the 3-sublattice ordering. (c, d) Excitation spectrum by linear spin-wave theory with dominant antiferromagnetic \mathcal{J}_x , for (c) $(\mathcal{J}_x, \mathcal{J}_y, \mathcal{J}_z) = (1, 0.4, 0)$ in AFO-AFD_y , and (d) $(\mathcal{J}_x, \mathcal{J}_y, \mathcal{J}_z) = (1, -0.4, 0)$ in AFO-FD_y .

sublattice structure persists for rather large \mathcal{J}_y and \mathcal{J}_z . Besides the antiferromagnetic order of the octupolar moment T^x , the dipolar moments are also antiferromagnetically ordered (Fig. 3a). The ordering of the local moments is constrained to either xy - or xz -plane depending on the magnitude of \mathcal{J}_y and \mathcal{J}_z , as in AFO-FD_y and AFO-AFD_z phases. The net magnetization of the dipolar moments in AFO-AFD phases is always zero, hence hidden to the thermodynamic measurements; but the 3-sublattice structure can manifest itself in the spin-wave excitations with 3 bands (see Fig. 3d). The gapless modes at Γ in Fig. 3c and d are accidental due to the extended degeneracy in the Ising limit and should be gapped when the magnon interactions are included.

Discussion.—It has been realized that a strong SOC could create a significant interaction between the magnetic multipole moments. The magnetic multipole orders have been proposed in several strong spin-orbit-coupled systems, e.g. the quadrupolar orders and the octupolar orders in ordered double perovskites [8]. The magnetic dipolar orders, being time reversally odd, are often concomitant with the magnetic octupolar orders. Since the former plays a dominant role in many magnetic measurements, it could complicate the interpretation of many experiments and the identification of the underlying octupolar orders. For the DO doublet on the triangular lattice, the lattice symmetry naturally distinguishes the octupole moments from the dipole ones and allows them to have independent structures.

The peculiar property of the DO doublets arises from

the wavefunction, and has little to do with the value of the total moment J . Any moment with $J > 1/2$ can potentially support a DO doublet as the CEF ground state doublet. There is no need to restrict J to be odd integer multiples of $3/2$. It gives a lot more room for the experimental discovery of DO doublets in the rare-earth triangular lattice materials. The experimental studies of the rare-earth triangular lattice materials have just started. The CEF ground states of most magnetic ions have not been understood. A systematic study of the CEFs will be of great interest. The magnetic properties of many materials in these families are not yet known, and a careful experimental investigation is highly needed.

To summarize, we propose a peculiar Kramers' doublet, namely, the dipole-octupole doublet, on a triangular lattice. We propose a rather simple model to describe the interaction between the dipole-octupole doublets and predict the hidden magnetic multipolar order and various unexpected properties associated with the multipolar order. In the future, we expect the unprecedented simplicity of the model and the absence of Monte Carlo sign problem will allow a direct comparison between theories, numerics, and experiments on these peculiar doublets.

Acknowledgments.—This work is supported by the Start-up Fund of Fudan University and the National Thousand-Young-Talents Program of People's Republic of China. Research at Perimeter Institute is supported by the Government of Canada through the Department of Innovation, Science and Economic Development Canada and by the Province of Ontario through the Ministry of Research, Innovation and Science.

* gangchen.physics@gmail.com

- [1] William Witczak-Krempa, Gang Chen, Yong Baek Kim, and Leon Balents, "Correlated quantum phenomena in the strong spin-orbit regime," *Annual Review of Condensed Matter Physics* **5**, 57–82 (2014).
- [2] Jeffrey G. Rau, Eric Kin-Ho Lee, and Hae-Young Kee, "Spin-orbit physics giving rise to novel phases in correlated systems: Iridates and related materials," *Annual Review of Condensed Matter Physics* **7**, 195–221 (2016).
- [3] Dmytro Pesin and Leon Balents, "Mott physics and band topology in materials with strong spin-orbit interaction," *Nature Physics* **6**, 376–381 (2010).
- [4] Lucile Savary and Leon Balents, "Quantum spin liquids," arXiv preprint arXiv:1601.03742 (2016).
- [5] G. Jackeli and G. Khaliullin, "Mott Insulators in the Strong Spin-Orbit Coupling Limit: From Heisenberg to a Quantum Compass and Kitaev Models," *Phys. Rev. Lett.* **102**, 017205 (2009).
- [6] Jeffrey G Rau, Eric Kin-Ho Lee, and Hae-Young Kee, "Generic spin model for the honeycomb iridates beyond the Kitaev limit," *Physical Review Letters* **112**, 077204 (2014).
- [7] Gang Chen and Leon Balents, "Spin-orbit effects in $\text{Na}_4\text{Ir}_3\text{O}_8$: A hyper-kagome lattice antiferromagnet," *Phys. Rev. B* **78**, 094403 (2008).
- [8] Gang Chen, Rodrigo Pereira, and Leon Balents, "Exotic phases induced by strong spin-orbit coupling in ordered double perovskites," *Phys. Rev. B* **82**, 174440 (2010).
- [9] Gang Chen and Leon Balents, "Spin-orbit coupling in d^2 ordered double perovskites," *Phys. Rev. B* **84**, 094420 (2011).
- [10] Yi-Ping Huang, Gang Chen, and Michael Hermele, "Quantum Spin Ices and Topological Phases from Dipolar-Octupolar Doublets on the Pyrochlore Lattice," *Phys. Rev. Lett.* **112**, 167203 (2014).
- [11] Yao-Dong Li and Gang Chen, "Octupolar quantum spin ice: controlling spinons in a U(1) quantum spin liquid," arXiv preprint 1607.02287 (2016).
- [12] Paolo Santini, Stefano Carretta, Giuseppe Amoretti, Roberto Caciuffo, Nicola Magnani, and Gerard H. Lander, "Multipolar interactions in f -electron systems: The paradigm of actinide dioxides," *Rev. Mod. Phys.* **81**, 807–863 (2009).
- [13] Premala Chandra, Piers Coleman, and Rebecca Flint, "Hastatic order in the heavy-fermion compound URu_2Si_2 ," *Nature* **493**, 621–626 (2013).
- [14] Premala Chandra, Piers Coleman, and Rebecca Flint, "Hastatic order in URu_2Si_2 : Hybridization with a twist," *Physical Review B* **91**, 205103 (2015).
- [15] Yuesheng Li, Gang Chen, Wei Tong, Li Pi, Juanjuan Liu, Zhaorong Yang, Xiaoqun Wang, and Qingming Zhang, "Rare-Earth Triangular Lattice Spin Liquid: A Single-Crystal Study of YbMgGaO_4 ," *Phys. Rev. Lett.* **115**, 167203 (2015).
- [16] Yao-Dong Li, Xiaoqun Wang, and Gang Chen, "Anisotropic spin model of strong spin-orbit-coupled triangular antiferromagnets," *Phys. Rev. B* **94**, 035107 (2016).
- [17] Yao Shen, Yao-Dong Li, Hongliang Wo, Yuesheng Li, Shoudong Shen, Bingying Pan, Qisi Wang, H. C. Walker, P. Steffens, M Boehm, Yiqing Hao, D. L. Quintero-Castro, L. W. Harriger, Lijie Hao, Siqin Meng, Qingming Zhang, Gang Chen, and Jun Zhao, "Spinon fermi surface in a triangular lattice quantum spin liquid YbMgGaO_4 ," arXiv preprint 1607.02615 (2016).
- [18] Joseph A. M. Paddison, Zhiling Dun, Georg Ehlers, Yao-hua Liu, Matthew B. Stone, Haidong Zhou, and Martin Mourigal, "Continuous excitations of the triangular-lattice quantum spin liquid YbMgGaO_4 ," arXiv preprint 1607.03231 (2016).
- [19] Yuesheng Li, Devashibhai Adroja, Pabitra K. Biswas, Peter J. Baker, Qian Zhang, Juanjuan Liu, Alexander A. Tsirlin, Philipp Gegenwart, and Qingming Zhang, " μSR evidence for the U(1) quantum spin liquid ground state in the triangular antiferromagnet YbMgGaO_4 ," arXiv preprint 1607.03298 (2016).
- [20] Yao-Dong Li, Yao Shen, Yuesheng Li, Jun Zhao, and Gang Chen, "The effect of spin-orbit coupling on the effective-spin correlation in YbMgGaO_4 ," arXiv preprint 1608.06445 (2016).
- [21] Stanislav S. Stoyko and Arthur Mar, "Ternary Rare-Earth Arsenides REZn_3As_3 ($\text{RE} = \text{La-Nd, Sm}$) and RECd_3As_3 ($\text{RE} = \text{La-Pr}$)," *Inorg. Chem* **50**, 1115211161 (2011).
- [22] A.T. Nientiedt and W. Jeitschko, "The Series of Rare Earth Zinc Phosphides RZn_3P_3 ($\text{R} = \text{Y, La-Nd, Sm, Gd-Er}$) and the Corresponding Cadmium Compound PrCd_3P_3 ," *Journal of Solid State Chemistry* **146**, 483

- (1999).
- [23] A. Yamada, N. Hara, K. Matsubayashi, K. Munakata, C. Ganguli, A. Ochiai, T. Matsumoto, and Y. Uwatoko, “Effect of pressure on the electrical resistivity of CeZn_3P_3 ,” *J. Phys.: Conf. Ser.* **215**, 012031 (2010).
 - [24] U. Arjun, K. Brinda, M. Padmanabhan, and R. Nath, “Magnetic properties of layered rare-earth oxycarbonates $\text{Ln}_2\text{O}_2\text{CO}_3$ ($\text{Ln}=\text{Nd}$, Sm , and Dy),” *Solid State Communications* **240**, 1–4 (2016).
 - [25] Kate A. Ross, Lucile Savary, Bruce D. Gaulin, and Leon Balents, “Quantum Excitations in Quantum Spin Ice,” *Phys. Rev. X* **1**, 021002 (2011).
 - [26] V. K. Anand, A. K. Bera, J. Xu, T. Herrmannsdörfer, C. Ritter, and B. Lake, “Observation of long-range magnetic ordering in pyrochlore $\text{Nd}_2\text{Hf}_2\text{O}_7$: A neutron diffraction study,” *Phys. Rev. B* **92**, 184418 (2015).
 - [27] E. Lhotel, S. Petit, S. Guitteny, O. Florea, M. Ciomaga Hatnean, C. Colin, E. Ressouche, M. R. Lees, and G. Balakrishnan, “Fluctuations and All-In All-Out Ordering in Dipole-Octupole $\text{Nd}_2\text{Zr}_2\text{O}_7$,” *Phys. Rev. Lett.* **115**, 197202 (2015).
 - [28] A. Bertin, P. Dalmas de Réotier, B. Fåk, C. Marin, A. Yaouanc, A. Forget, D. Sheptyakov, B. Frick, C. Ritter, A. Amato, C. Baines, and P. J. C. King, “ $\text{Nd}_2\text{Sn}_2\text{O}_7$: An all-in all-out pyrochlore magnet with no divergence-free field and anomalously slow paramagnetic spin dynamics,” *Phys. Rev. B* **92**, 144423 (2015).
 - [29] J. Xu, V. K. Anand, A. K. Bera, M. Frontzek, D. L. Abernathy, N. Casati, K. Siemensmeyer, and B. Lake, “Magnetic structure and crystal-field states of the pyrochlore antiferromagnet $\text{Nd}_2\text{Zr}_2\text{O}_7$,” *Phys. Rev. B* **92**, 224430 (2015).
 - [30] M. Ciomaga Hatnean, M. R. Lees, O. A. Petrenko, D. S. Keeble, G. Balakrishnan, M. J. Gutmann, V. V. Klekovkina, and B. Z. Malkin, “Structural and magnetic investigations of single-crystalline neodymium zirconate pyrochlore $\text{Nd}_2\text{Zr}_2\text{O}_7$,” *Phys. Rev. B* **91**, 174416 (2015).
 - [31] S. Petit, E. Lhotel, B. Canals, M. Ciomaga Hatnean, J. Ollivier, H. Mutka, E. Ressouche, A.R. Wildes, M.R. Lees, and G. Balakrishnan, “Observation of magnetic fragmentation in spin ice,” *Nature Physics* **advance online publication** (2016), 10.1038/nphys3710.
 - [32] S. Pokrzywnicki, “Analysis of the Magnetic Susceptibility of CdYb_2S_4 spinel by Means of the Crystal Field Method,” *phys. stat. sol. (b)* **71**, K111 (1975).
 - [33] A. Bertin, Y. Chapuis, P. Dalmas de Rotier, and A. Yaouanc, “Crystal electric field in the $\text{R}_2\text{Ti}_2\text{O}_7$ pyrochlore compounds,” *Journal of Physics: Condensed Matter* **24**, 256003 (2012).
 - [34] Akihiro Koda, Ryosuke Kadono, Kazuki Ohishi, Shanta R. Saha, Wataru Higemoto, Shigeki Yonezawa, Yuji Muraoka, and Zenji Hiroi, “Anomalous Magnetic Phase in an Undistorted Pyrochlore Oxide $\text{Cd}_2\text{Os}_2\text{O}_7$ Induced by Geometrical Frustration,” *Journal of the Physical Society of Japan* **76**, 063703 (2007).
 - [35] J. Yamaura, K. Ohgushi, H. Ohsumi, T. Hasegawa, I. Yamauchi, K. Sugimoto, S. Takeshita, A. Tokuda, M. Takata, M. Udagawa, M. Takigawa, H. Harima, T. Arima, and Z. Hiroi, “Tetrahedral Magnetic Order and the Metal-Insulator Transition in the Pyrochlore Lattice of $\text{Cd}_2\text{Os}_2\text{O}_7$,” *Phys. Rev. Lett.* **108**, 247205 (2012).
 - [36] J. Lago, I. Živković, B. Z. Malkin, J. Rodríguez Fernández, P. Ghigna, P. Dalmas de Réotier, A. Yaouanc, and T. Rojo, “ CdEr_2Se_4 : A New Erbium Spin Ice System in a Spinel Structure,” *Phys. Rev. Lett.* **104**, 247203 (2010).
 - [37] Romain Sibille, Elsa Lhotel, Vladimir Pomjakushin, Chris Baines, Tom Fennell, and Michel Kenzelmann, “Candidate Quantum Spin Liquid in the Ce^{3+} Pyrochlore Stannate $\text{Ce}_2\text{Sn}_2\text{O}_7$,” *Phys. Rev. Lett.* **115**, 097202 (2015).
 - [38] See the Supplementary information.
 - [39] Gang Chen, (2016), Unpublished.
 - [40] Weeje Cho and Steven A. Kivelson, “Necessity of Time-Reversal Symmetry Breaking for the Polar Kerr Effect in Linear Response,” *Phys. Rev. Lett.* **116**, 093903 (2016).
 - [41] R. G. Melko, A. Paramekanti, A. A. Burkov, A. Vishwanath, D. N. Sheng, and L. Balents, “Supersolid Order from Disorder: Hard-Core Bosons on the Triangular Lattice,” *Phys. Rev. Lett.* **95**, 127207 (2005).
 - [42] Stefan Wessel and Matthias Troyer, “Supersolid Hard-Core Bosons on the Triangular Lattice,” *Phys. Rev. Lett.* **95**, 127205 (2005).
 - [43] Daisuke Yamamoto, Giacomo Marmorini, and Ipppei Danshita, “Quantum Phase Diagram of the Triangular-Lattice XXZ Model in a Magnetic Field,” *Phys. Rev. Lett.* **112**, 127203 (2014).
 - [44] Daniel Sellmann, Xue-Feng Zhang, and Sebastian Eggert, “Phase diagram of the antiferromagnetic XXZ model on the triangular lattice,” *Phys. Rev. B* **91**, 081104 (2015).

I. Dipole-octupole doublet

We consider the general wavefunctions of a DO doublet that are linear superpositions of the J^z states with odd integer multiples of $3/2$,

$$|\Psi_+\rangle = \sum_{n_1>0} a_{n_1} |J^z = \frac{3n_1}{2}\rangle + \sum_{n_2<0} a_{n_2} |J^z = \frac{3n_2}{2}\rangle, \quad (7)$$

$$|\Psi_-\rangle = \sum_{n_1>0} (-)^{\frac{n_1+1}{2}} a_{n_1}^* |J^z = -\frac{3n_1}{2}\rangle + \sum_{n_2<0} (-)^{\frac{n_2+1}{2}} a_{n_2}^* |J^z = -\frac{3n_2}{2}\rangle, \quad (8)$$

in which $|\Psi_-\rangle$ is simply obtained from $|\Psi_+\rangle$ by a time reversal operation. Here, both n_1 and n_2 are odd integers by definition, and we assume the wavefunctions have been properly normalized. Using the definition of the effective spin operator in the main text, we can relate the effective spin τ^μ with the total moment J^μ as follows

$$\tau^z \propto PJ^zP, \quad (9)$$

$$\tau^+ \propto P(J^+)^{3n_1}P \quad \text{or} \quad \propto P(J^-)^{3|n_2|}P, \quad (10)$$

$$\tau^- \propto P(J^-)^{3n_1}P \quad \text{or} \quad \propto P(J^+)^{3|n_2|}P, \quad (11)$$

where $P = |\Psi_+\rangle\langle\Psi_+| + |\Psi_-\rangle\langle\Psi_-|$ is the projection operator that projects onto the DO doublet manifold. In Eq. (10) and Eq. (11), the lowest order in J^\pm is $(J^\pm)^3$. Although the magnetic field couples linearly to J^μ , only τ^z component survives after we restrict the magnetic field coupling to the DO doublet. The octupole moment τ^x , however, can couple to the magnetic field in the cubic order.

II. Space group symmetry

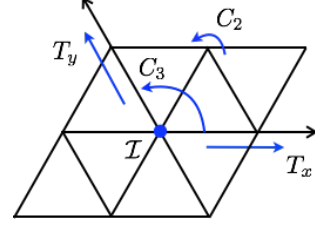


FIG. 4. The generators of the space group symmetry for a single triangular layer.

As we have explained in the main text, we only need to keep the space group symmetry generators of the $R\bar{3}m$ or $P6_3mmc$ space group. Within the triangular layer, both $R\bar{3}m$ and $P6_3mmc$ space groups give the same list of symmetry generators. As we show in Fig. 4, we have the three-fold rotation, C_3 , the two-fold rotation, C_2 , the inversion, I , and two lattice translations, T_x and T_y . Under the symmetry operation, the total moment J^μ transforms as

$$\begin{cases} C_3 : J_{\mathbf{r}}^z \rightarrow J_{C_3(\mathbf{r})}^z, & J_{\mathbf{r}}^+ \rightarrow e^{-i\frac{2\pi}{3}} J_{C_3(\mathbf{r})}^+, & J_{\mathbf{r}}^- \rightarrow e^{i\frac{2\pi}{3}} J_{C_3(\mathbf{r})}^-, \\ C_2 : J_{\mathbf{r}}^z \rightarrow -J_{C_2(\mathbf{r})}^z, & J_{\mathbf{r}}^+ \rightarrow e^{i\frac{2\pi}{3}} J_{C_2(\mathbf{r})}^-, & J_{\mathbf{r}}^- \rightarrow e^{-i\frac{2\pi}{3}} J_{C_2(\mathbf{r})}^+, \\ I : J_{\mathbf{r}}^z \rightarrow J_{I(\mathbf{r})}^z, & J_{\mathbf{r}}^+ \rightarrow J_{I(\mathbf{r})}^+, & J_{\mathbf{r}}^- \rightarrow J_{I(\mathbf{r})}^-, \\ T_x : J_{\mathbf{r}}^z \rightarrow J_{T_x(\mathbf{r})}^z, & J_{\mathbf{r}}^+ \rightarrow J_{T_x(\mathbf{r})}^+, & J_{\mathbf{r}}^- \rightarrow J_{T_x(\mathbf{r})}^-, \\ T_y : J_{\mathbf{r}}^z \rightarrow J_{T_y(\mathbf{r})}^z, & J_{\mathbf{r}}^+ \rightarrow J_{T_y(\mathbf{r})}^+, & J_{\mathbf{r}}^- \rightarrow J_{T_y(\mathbf{r})}^-, \end{cases} \quad (12)$$

Using the relations in Eqs. (9-11), we obtain the symmetry properties of the pseudospin τ^μ .

III. The transformation for the pseudospin

In the transformation that we did to eliminate the crossing coupling between τ^y and τ^z , we choose the θ variable such that

$$\sin 2\theta = \frac{2J_{yz}}{[(J_y - J_z)^2 + (2J_{yz})^2]^{\frac{1}{2}}} \quad (13)$$

$$\cos 2\theta = \frac{J_y - J_z}{[(J_y - J_z)^2 + (2J_{yz})^2]^{\frac{1}{2}}}, \quad (14)$$

and, the new couplings in the reduced model are given as

$$\begin{aligned} \mathcal{J}_x &= J_x, \\ \mathcal{J}_y &= \frac{1}{2} [J_y + J_z + (J_y - J_z) \cos(2\theta)] \end{aligned} \quad (15)$$

$$+ 2J_{yz} \sin(2\theta)], \quad (16)$$

$$\begin{aligned} \mathcal{J}_z &= \frac{1}{2} [J_y + J_z - (J_y - J_z) \cos(2\theta) \\ &\quad - 2J_{yz} \sin(2\theta)]. \end{aligned} \quad (17)$$

IV. Mean field theory in the ferro-octupolar ordered regime

Starting with the model in Eq. (4), we apply mean field decoupling of terms quadratic in T^μ by neglecting their fluctuations,

$$T_{\mathbf{r}}^\mu T_{\mathbf{r}'}^\mu \rightarrow \langle T_{\mathbf{r}}^\mu \rangle T_{\mathbf{r}'}^\mu + T_{\mathbf{r}}^\mu \langle T_{\mathbf{r}'}^\mu \rangle - \langle T_{\mathbf{r}}^\mu \rangle \langle T_{\mathbf{r}'}^\mu \rangle. \quad (18)$$

For the ferromagnetic order, we can assume a site-independent ansatz, and define $m^\mu \equiv \langle T_{\mathbf{r}}^\mu \rangle$. This gives us the mean-field Hamiltonian,

$$H_{\text{MF}} = 6 \sum_{\mathbf{r}} [\mathcal{J}_x m^x T_{\mathbf{r}}^x + \mathcal{J}_y m^y T_{\mathbf{r}}^y + \mathcal{J}_z m^z T_{\mathbf{r}}^z]$$

$$-h \sum_{\mathbf{r}} [\cos \theta T_{\mathbf{r}}^z + \sin \theta T_{\mathbf{r}}^y]. \quad (19)$$

This Hamiltonian can be diagonalized, and m^μ can be solved self-consistently. For dominant \mathcal{J}_x , we may further assume $m^y = m^z = 0$.

At $T = 0$ and $h = 0$, it is obvious that $m^x = 1/2$. For finite T , the self-consist equation is given by $m^x = \frac{1}{2} \tanh \frac{3m^x}{T}$. Since T^x does not couple to h linearly, an infinitesimal h would not alter the form of this self-consistent equation. It can be shown that $m^y \sim \frac{\tanh(3m^x/T)h}{2m^x}$ and $m^z \sim \frac{\tanh(3m^x/T)h}{2m^x}$, hence a constant χ^{zz} below T_c .

V. Mean field theory in the antiferro-octupolar ordered regime

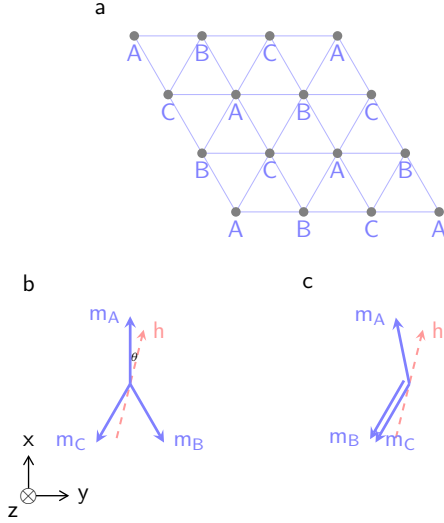


FIG. 5. (a) The 3-sublattice structure on the triangular lattice. (b), (c) Two mean-field ansätze of the magnetization vectors for dominant antiferromagnetic \mathcal{J}_x . These patterns are obtained by mimicking the supersolid order obtained for the XXZ model [41–44]. The inset is the coordinate system in the pseudospin space.

When the dominant exchange is antiferromagnetic, we assume a 3-sublattice structure (see Fig. 5) for the mean-field ansatz, by defining the magnetization for each sublattice, $\mathbf{m}_i = \langle \mathbf{T}_i \rangle$, where $i = A, B, C$. This assumption is consistent with results in the XXZ model. As a result,

the mean field Hamiltonian reads

$$\begin{aligned} H_{\text{MF}} = & 3 \sum_{\mathbf{r} \in A} \sum_{\mu} [\mathcal{J}_{\mu} (m_B^{\mu} + m_C^{\mu}) T_{\mathbf{r}}^{\mu}] \\ & + 3 \sum_{\mathbf{r} \in B} \sum_{\mu} [\mathcal{J}_{\mu} (m_C^{\mu} + m_A^{\mu}) T_{\mathbf{r}}^{\mu}] \\ & + 3 \sum_{\mathbf{r} \in C} \sum_{\mu} [\mathcal{J}_{\mu} (m_A^{\mu} + m_B^{\mu}) T_{\mathbf{r}}^{\mu}] \\ & - h \sum_{\mathbf{r}} [\cos \theta T_{\mathbf{r}}^z + \sin \theta T_{\mathbf{r}}^y]. \end{aligned} \quad (20)$$

To reduce the number of free parameters, we further constraint the magnetization vectors to form patterns depicted in Fig. 5b,c. The Hamiltonian on each sublattice can now be diagonalized separately, and we solve for \mathbf{m}_i self-consistently. We determine the phase diagram by comparing the mean-field ground state energy between the two possible patterns of orderings and measuring the suppression of $\langle T^x \rangle$.

VI. Linear spin wave theory

Our mean field theory gives the magnetization vectors for different parameter regimes. Within such phases, there is a stable magnetic ordering, therefore spin wave excitations are well-defined. Using neutron scattering one can measure the spin wave spectrum, as an indirect probe of the ground state.

Suppose the magnetization on site i is given by \mathbf{m}_i , we introduce the Holstein-Primakoff representation for the pseudospin- $\frac{1}{2}$ operators,

$$\mathbf{T}_i \cdot \hat{\mathbf{m}}_i = \frac{1}{2} - a_i^{\dagger} a_i, \quad (21)$$

$$\mathbf{T}_i \cdot \hat{\mathbf{z}}_i = \frac{1}{2} (a_i + a_i^{\dagger}), \quad (22)$$

$$\mathbf{T}_i \cdot [\hat{\mathbf{m}}_i \times \hat{\mathbf{z}}_i] = \frac{1}{2i} (a_i - a_i^{\dagger}), \quad (23)$$

where $\hat{\mathbf{m}}_i$ is the unit vector parallel to \mathbf{m}_i , and $\hat{\mathbf{z}}_i$ is a unit vector perpendicular to $\hat{\mathbf{m}}_i$. In this representation, the Bloch Hamiltonian has the form

$$H_{\text{HP}} = \sum_{\mathbf{k} \in \text{BZ}'} (A_{\mathbf{k}}^{\dagger}, A_{-\mathbf{k}}) \begin{pmatrix} F_{\mathbf{k}} & G_{\mathbf{k}}^{\dagger} \\ G_{\mathbf{k}} & F_{-\mathbf{k}} \end{pmatrix} \begin{pmatrix} A_{\mathbf{k}} \\ A_{-\mathbf{k}}^{\dagger} \end{pmatrix}, \quad (24)$$

where $A_{\mathbf{k}} = (a_{1\mathbf{k}}, \dots, a_{n\mathbf{k}})$ is the vector of boson annihilation operators, the subindices $1 \dots n$ label the n sublattices of the magnetic unit cell, and BZ' is the magnetic Brillouin zone. $F_{\mathbf{k}}$ and $G_{\mathbf{k}}$ are 2×2 matrices and depend on the mean field magnetizations. The Bloch Hamiltonian is diagonalized by the standard Bogoliubov transformation, giving the spectrum of Holstein-Primakoff bosons plotted in Fig. 1 and Fig. 3.